The Scientific Temper (2024) Vol. 15 (2): 2190-2198
E-ISSN: 2231-6396, ISSN: 0976-8653
Doi: 10.58414/SCIENTIFICTEMPER.2024.15.2.31
https://scientifictemper.com/

RESEARCH ARTICLE

Study and optimization of process parameters for deformation machining stretching mode

P. L. Parmar*, P. M. George

Abstract

Monolithic thin-structure parts with intricate geometric designs are employed in a variety of aeronautical, medical, marine, and automotive applications, which include the moldlines of the fuselage, turbine blades, impellers, avionic shelves, irregular fins, prostheses, bone and joint support, and skull plates. The deformation machining process is the solution to this challenging and difficult-to-manufacture high-quality components with intricate narrow geometries at competitive prices. The aim of the present study is to assess the effect of process parameters of the deformation machining process wherein a thin, floor-like structure is created by milling and is then formed using a single-point incremental forming tool. Investigation involves the design and development of tooling required for the process followed by feasibility checking of the process. To examine the impact of different process parameters on the process response, the experiments were carried out using the design of experiments. The findings of this study indicate that different process parameters, including spindle speed, tool diameter, incremental step depth, and feed rate, have a substantial impact on the process response, like thickness, surface finish, and hardness. Uneven and non-uniform surface patterns during SEM indicate that it is needed to examine the impact of process parameters. This research involves the feasibility study of a new hybrid technique of deformation machining. Conventionally, a metallic structure is produced by joining various components through welding or by fastening. These methods require additional expenditure on equipment, storage, floor space, human resources, etc., with higher lead time. Joining increases weight and reduces fatigue strength. The creation of monolithic structures can eliminate all these disadvantages.

Keywords: Deformation machining, Surface roughness, Hardness, Grey relation analysis, Analysis of Variance.

Introduction

Thin metallic monolithic structures made of aluminum alloys like Al 6061 are widely utilized in the aerospace sector in various application areas, including aircraft. Such thin components are machined using a deformation machining method, which can replace a significant amount of assembly work. The strength, formability, and overall functionality of the part are all impacted by variations in thickness caused by deformation zones during metal forming procedures. Jeswiet and Filice (Filice *et al*., 2002) carried out a capability analysis on a machine tool that was specifically created. Due to its highly localized plastic deformation, incremental forming has improved formability as compared to other traditional forming techniques (J. Smith *et al*., 2013)(Jeswiet, Micari, *et al*., 2005). The objective of the study is to examine whether the process and necessary tools are practical. The moving tool that is numerically controlled deforms the sheet (Jeswiet & Young, 2005). By modifying the standard spinning and shear forming, localized deformation can be achieved (Silva *et al*., 2009). A complex product like a personalized ankle brace is also manufactured using the single-point incremental forming process. The low accuracy and process lag should still be regarded as open issues (Ambrogio *et al*., 2005). There is still work to be done in the areas of process time, forces created during the process, produced component shape, microstructural analysis, and responses of various materials.

Preliminary findings in the feasibility analysis of the method for deformation machining stretching mode are encouraging and suggest a wide variety of potential industrial applications. Thin features, such as pins, walls, or even floors, are produced by different machining operations starting with plate stock. The thin portions are then deformed in one of two ways—either bending or stretching—using

Gujarat Technological University, Ahmedabad, Gujarat, India.

***Corresponding Author:** P. L. Parmar, Gujarat Technological University, Ahmedabad, Gujarat, India, E-Mail: ap_pradhuman@gtu.edu.in

How to cite this article: Parmar, P. L., George, P. M. (2024). Study and optimization of process parameters for deformation machining stretching mode. The Scientific Temper, **15**(2):2190-2198.
Doi: 10.58414/SCIENTIFICTEMPER.2024.15.2.31

Source of support: Nil

Conflict of interest: None.

Received: 04/04/2024 **Accepted:** 05/05/2024 **Published** : 15/06/2024

a forming tool and the single point incremental forming (SPIF) technique. Making intriguing features that are lighter, thinner, or less expensive as compared to the structures they replace is feasible by alternating between the machining tool and the deformation tool. Additionally, geometries that would be challenging or impossible to build using other procedures can be produced (K. S. Smith *et al*., 2009). In the aerospace industry, thin structures are frequently utilized. Force data indicates that the operation can be completed using current machine tools, and the amount of the deformation forces is comparable to the cutting forces. The possibilities for the thin wall/floor structure are essentially unlimited (G. S. Smith *et al*., 2007). It can be selectively and gradually bent along its transverse direction to produce components like an impeller blade or anything similar, or it can be bent to form any type of C-channel, overhang or lip, U-channel, or other shapes.

Unlike normal milling, the DM technique does not offer precise tolerances. This might be because of springback and regional variations in the characteristics of the material, which affect yield strength and cause springback. However, it was discovered that the components made using this technique were less repeatable than those made using conventional sheet metal bending but more repeatable when compared to similar components made using SPIF (Agrawal *et al*., 2012). Springback, residual stresses, and elastic deformation highly localized yielding are other elements that can impair the process's capacity to repeat dimensions. One new area of study that could be explored is the part residual stressors play in this process (Singh & Agrawal, 2014). The elastic springback is significantly influenced by the feed rate, as well as dimensional characteristics, including wall thickness, bent angle, and H/L (Height/Length) ratio. Future research will focus on creating connections between various elastic springback characteristics and establishing a comprehensive experimental model that includes a wide variety of parameters at various levels for reliable springback prediction (Singh & Agrawal, 2015a). The fatigue life, corrosion resistance, strength, and total life of components are all significantly impacted by residual stresses. Deformation machining causes residual stresses to be produced in the component (Singh & Agrawal, 2015b). Deformation machining and SPIF were found to significantly reduce deformation forces compared to conventional forming. This research offers the first ideas for commercializing the method as an alternative to traditional shaping (Singh & Agrawal, 2016a).

A variable thin-section machining compensating approach was used before incremental forming to obtain the desired formed thickness and substantially uniform profiles throughout the forming depth. The generated monolithic components' formability and strength would likely be improved as a result. Extension of structural thinning and compensating to different profiles and geometries with different forming angles would be a future study (Singh & Agrawal, 2016b). The geometry was shown to be a key factor in determining how the shape of the produced component affected the average resulting forces (Singh & Agrawal, 2017). In contrast to physical characteristics like floor size and floor thickness, process variables like forming angle, incremental depth, and forming tool diameter have a considerable impact on the average radial error in DM stretching mode components. Finding methods and procedures to do away with geometrical errors to attain a good level of accuracy could be the focus of future work in this field, and for this, the process still has to be researched for advancement (Singh & Agrawal, 2018). In comparison to helical tool paths, profile tool paths are observed to exhibit increased surface roughness and thinning (S. Smith & Dvorak, 1998). A study was conducted by Ham and Jeswiet (Tlusty *et al*., 1996) to determine how different process variables affected the forming angle. Moreover, CapeceMinutolo *et al*. (Malhotra *et al*., 2010) used the maximum forming wall angle to successfully assess the formability of both cones and truncated pyramids. Bhattacharya *et al*. (Jagtap *et al*., 2015) did a series of studies and discovered that formable angle 1st rises and then falls with step-down size. In 46 experiments, Ham (Ambrogio, Gagliardi, Bruschi, *et al*., 2013) used five factors—sheet thickness, material type, step-down size, tool size, and formed shape—across five different material types and sheet thicknesses. Hagan and Jeswiet (Silva *et al*., 2009) examined how several forming factors, including spindle speed and step-down size, affected surface roughness in the ISF process. A SPIF case study was used by Powers *et al*. (Jeswiet, Duflou, *et al*., 2005) to investigate the surface morphology. The thickness and material type, tool speed, tool path shape, incremental depth, tool diameter, spring back compensation, multi-stage forming, and feature compensation are some of the defined process parameters in SPIF (Ambrogio, Gagliardi, & Filice, 2013) (Azaouzi & Lebaal, 2012). The concept of a tool path for greater dimensional accuracy and improved surface quality is presented by Bhattacharya *et al*. (Bhattacharya *et al*., 2011). A thickness variation study for the process was carried out shows promising results (Parmar & George, 2021). For both academic researchers and industry users, geometric precision for ISF products continues to be one of the main problems at the moment. In particular, the geometric accuracy, residual stress, hardness, surface quality, thickness fluctuations, and material formability are impacted by decisions made in relation to tool path techniques.

Experiment Work

This research involves examining how process variables like spindle speed, incremental step depth, feed rate, and tool diameter affect process responses like thickness variation, surface roughness, and hardness for deformation machining of Al 6061. Empirical mathematical models for thickness

Table 1: Process parameters and their levels for machining thin floor

Parameters/Factors	*Levels*
Tool material	Tungsten carbide
Tool diameter	12 mm
Spindle speed	60 m/minute
Transverse feed	0.5 m/minute
Depth of cut	0.5 mm

Table 2: Process parameters and their levels for forming

Parameters/Factors	*Levels*
Spindle speed, A	40, 60, 80 rpm
Feed rate, B	2000, 4000, 6000 mm/min
Tool diameter, C	6, 8, 10 mm
Incremental step depth, D	0.08, 0.10, 0.12 mm

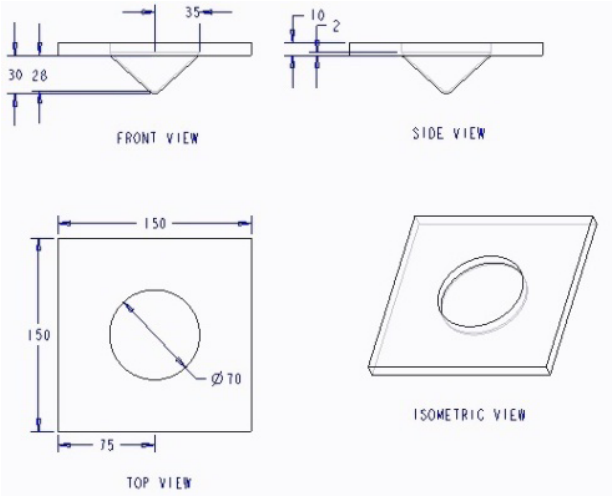

Figure 1: Component's drawing

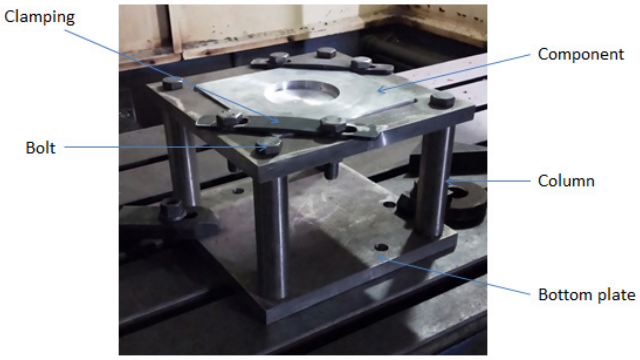

Figure 2: DM stretching model setup

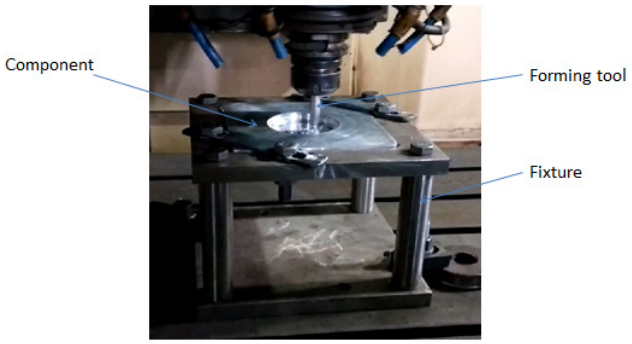

Figure 3: DM stretching mode operation

variation, surface roughness, and hardness have been built using the experimental data and can be used to anticipate reactions. To determine the significant parameters and their interaction, ANOVA tests have been run. To determine the optimum process parameters, the grey relational analysis (GRA) as a multi-objective optimization approach is utilized.

On the TML VMC650 machine, experiments were conducted for the research work. To investigate the impact of incremental step depth, spindle speed, feed rate, and tool diameter on the process responses of thickness variation, surface roughness, and hardness for deformation machining of Al 6061 experiments were organized using a fractional factorial experimental design. Both the machining and the forming were done using TAL Manufacturing Solutions Ltd.'s machining center V-650. In NX 12 manufacturing, a tool travel program was created according to the path needed for cutting and forming as the DM stretching mode combines machining and forming, two processes. Following a review of the concrete literature, four variable parameters were chosen with the range for the forming. An end mill made of solid carbide was used to machine a thin floor. Using HCHCR material, forming tools are created as SPIF tools. As shown in Figures 1 and 2, the process setup comprises four columns, a base plate, a top plate, and clamping using nuts and bolts. The thin-walled floor was processed to achieve a conical shape up to a depth of 30 mm. A thin floor with a 2 mm thickness and 70 mm diameter is produced by milling a 150×150×10 mm aluminum alloy Al 6061 plate. Using a single-point incremental forming tool, this milled thin floor was created to a depth of 30 mm (Figure 3). For the 150×150×10 mm component, the top plate was milled about 8 mm deep, and an 80 mm diameter bore was made in the center to provide the area needed for constructing the floor thickness.

DoE is a helpful technique to pinpoint key variables influencing the answer as well as to establish empirical relationships between distinct responses and variables. In essence, the knowledge aids in process parameter optimization to produce superior performance characteristics. The experimental run is carried out using a 2^{4-1} fraction factorial scheme, as stated in Tables 1-3.

After the experimental run was successfully completed, specimens were examined for thickness, surface quality, and hardness. The results are displayed in Table 3. Analysis

Figure 4: Specimens formed by deformation machining

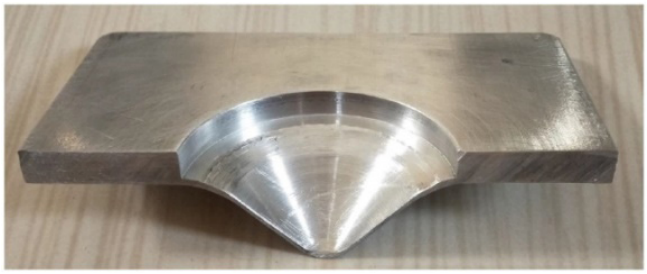

Figure 5: Cut a section of a specimen

of Variance (ANOVA) is used to identify the important variables and determine how much of an impact they have on thickness. The parametric effect on response is investigated using the main effect plot and the interaction plot. To explore the impact of process parameters, a total of 12 components were made in accordance with the 2^{4-1} DoE plan. Components were cut symmetrically, and thickness was determined at 2 mm intervals up to its complete depth, or 30 mm (Figures 4 and 5).

Results And Discussion

To avoid any systematic error, four center points were taken with a total of 12 experimental runs. Analysis through the ANOVA method is done to test the significance of the model coefficients and a regression model is generated. Tables 4, 5, and 6 show ANOVA table for thickness variation, surface roughness, and hardness.

Figure 6 shows the thickness measurement using CMM, whereas Figures 7 and 8 show the surface roughness and hardness measurement, respectively.

Thickness Variation

ANOVA was used to examine the average thickness data to pinpoint the important variables influencing the performance metrics. After cutting, a coordinate measuring machine (CMM) was applied to determine the variance in wall thickness at different forming depths. The average

Table 3: Experimental data and responses

S. No./ Factors	*A*	*B*	*C*	*D*	*Average thickness (mm)*	*Ra (μm)*	*Hardness (HV)*
1	40	2000	0.08	6	1.738	1.941	118
2	80	2000	0.08	10	1.690	2.429	116
3	40	6000	0.08	10	1.711	3.665	112
4	80	6000	0.08	6	1.721	3.103	107
5	40	2000	0.12	10	1.672	3.195	107
6	80	2000	0.12	6	1.681	3.484	106
7	40	6000	0.12	6	1.702	3.285	104
8	80	6000	0.12	10	1.668	3.686	105
9	60	4000	0.1	8	1.712	2.892	114
10	60	4000	0.1	8	1.714	2.962	115
11	60	4000	0.1	8	1.715	2.922	115
12	60	4000	0.1	8	1.710	2.974	114

Figure 6: Thickness measurement using CMM

thickness was then considered for additional analysis (Figures 9 and 10). The thickness at different depths

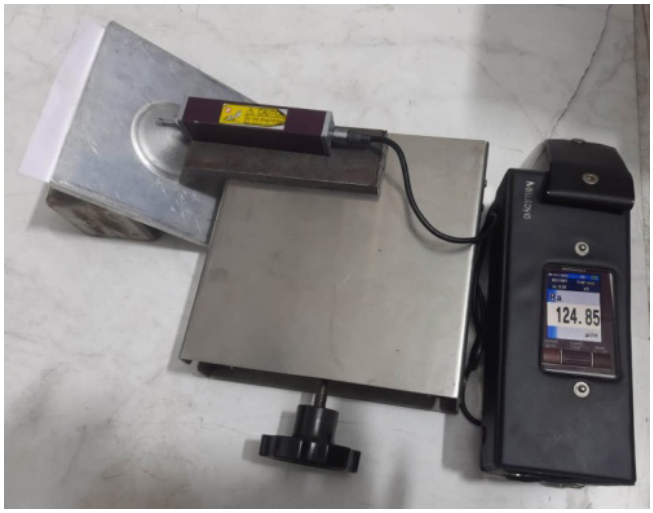

Figure 7: Surface tester measuring surface roughness

Figure 8: Hardness tester DoHP100

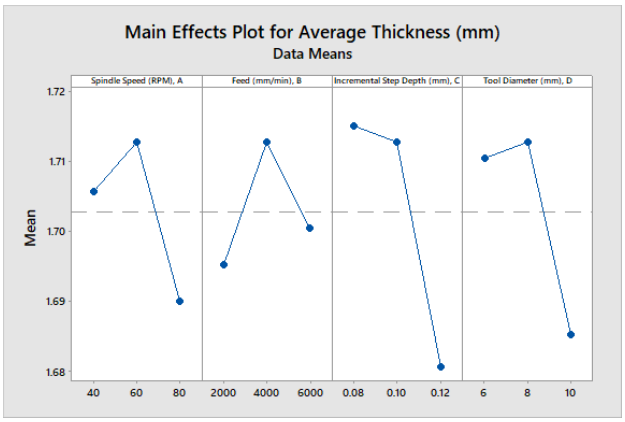

Figure 9: Main effect plot for factors A, B, C, and D

indicates that the bending zone forms first and is followed by thinning at the beginning of the forming process. The parameters under investigation include tool diameter, feed rate, incremental step depth, and spindle speed of these, incremental step depth has the highest effect on thickness variation. Thickness variation rises with each step's depth. The next most important factor influencing thickness variation is tool diameter, followed by spindle speed and feed. ANOVA is provided for average thickness in Table 4. The model that fits is provided below:

Average Thickness (mm) = 1.9075 - 0.001312 A - 0.000001 B- 1.100 C-0.00875 D+0.000001 A*B + 0.00406 A*C+0.000041 A*D+0.01488 Ct Pt

Surface Roughness

According to the analysis and the developed model, the incremental step depth, spindle speed, feed rate, and tool diameter are the four parameters that have the greatest influence on surface roughness in ascending order. The

Table 4: Anova for average thickness

Source	*DF*	*Adj SS*	*Adj MS*	*F-value*	*p-value*
Model	8	0.004833	0.000604	122.87	0.001
Linear	4	0.004172	0.001043	212.16	0.001
A	1	0.000496	0.000496	100.91	0.002
B	1	0.000055	0.000055	100.91	0.044
C	1	0.002346	0.002346	11.21	0.000
D	1	0.001275	0.001275	477.18	0.001
2-Way Interactions	3	0.000070	0.000070	259.35	0.116
A*B	1	0.000028	0.000028	4.77	0.097
A*C	1	0.000021	0.000021	5.72	0.130
A*D	1	0.000021	0.000021	4.30	0.130
Curvature	1	0.000590	0.000590	4.30	0.002
Error	3	0.000015	0.000005	120.01	
Total	11	0.004848			

Table 5: Anova for average Ra

Source	*DF*	*Adj SS*	*Adj MS*	*F-Value*	*p-value*
Model	8	2.71596	0.339495	240.04	0.000
Linear	4	1.90949	0.477373	337.53	0.000
A	1	0.04743	0.047432	33.54	0.010
B	1	0.90451	0.904513	639.53	0.000
C	1	0.78877	0.788768	557.70	0.000
D	1	0.16878	0.168781	119.34	0.002
2-Way Interactions	3	0.73735	0.245782	173.78	0.001
A*B	1	0.10998	0.109981	77.76	0.003
A*C	1	0.07296	0.072962	51.59	0.006
A*D	1	0.55440	0.554405	391.99	0.000
Curvature	1	0.06912	0.069123	48.87	0.006
Error	3	0.00424	0.001414		
Total	11	2.72021			

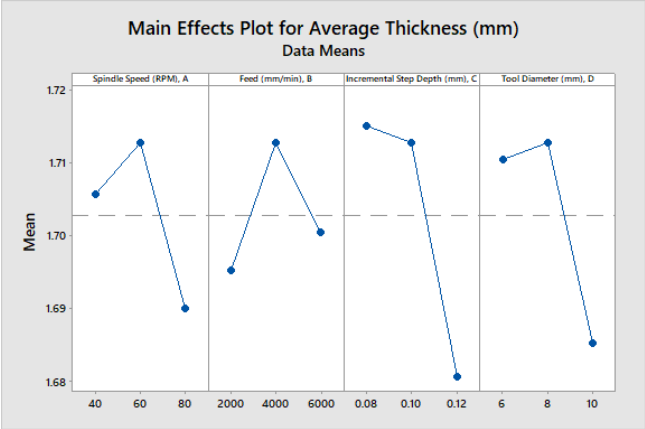

Figure 10: Main effect plot for average thickness

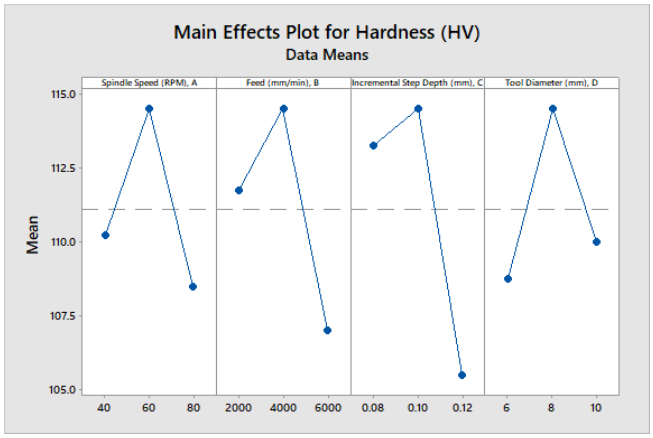

Figure 11: Main effect plot for hardness

surface roughness reduces as the feed rate increases. Surface roughness reductions with decreasing feed rate and spindle speed values. The average Ra's ANOVA is displayed in Table 5, and the corresponding regression model is provided below:

Average Ra(μm)=-2.386+0.04435A+0.000344 B+1.38C+0.4675D-0.000003A*B+0.2387 A*C-0.006581 A*D - 0.1610 Ct Pt

Hardness

From the main affect plot (Figure 11), it is concluded that at a higher value of incremental step depth, hardness decreases. Incremental step depth is the most significant parameter affecting the hardness with a *p-value* of 0.060 followed by feed rate having a *p-value* of 0.186. The main effect plot for hardness also indicates that lower values of parameters give higher values of hardness. ANOVA of the hardness model is given in Table 6. The hardness model is given below:

Hardness (HV) = 164.2 - 0.525 A - 0.00100 B - 325 C - 1.75 D–0.000003 A*B+2.19 A*C+0.0344 A*D

Table 6: ANOVA for hardness

Source	*DF*	*Adj SS*	*Adj MS*	*F-value*	*p-value*
Model	8	195.875	27.982	1.58	0.346
Linear	4	174.500	43.625	2.46	0.203
A	1	6.125	6.125	0.34	0.589
B	1	45.125	45.125	2.54	0.186
C	1	120.125	120.125	6.76	0.060
D	1	3.125	3.125	0.18	0.696
2-Way Interactions	3	21.375	7.125	0.40	0.761
A*B	1	0.125	0.125	0.01	0.937
A*C	1	6.125	6.125	0.34	0.589
A*D	1	15.125	15.125	0.85	0.408
Curvature	1	70.042	70.042	210.12	0.001
Error	3	1.000	0.333		
Total	11	266.917			

Multi-Objective Optimization

Since the goal would be to simultaneously maximize and minimize several responses, it is frequently not possible to optimize the researched process parameters for just one reaction. The various response process improvements are converted into a single objective issue using GRA. The best possible parameter combination will be determined by evaluating the highest GRG. Under these circumstances, the normalized value is computed (Table 7) using the following equation:

- Higher-the-better

$$x_i^*(k) = \frac{x_i^0(k) - \min x_i^0(k)}{\max x_i^0(k) - \min x_i^0(k)}$$

- Lower-the-better

$$x_i^*(k) = \frac{\max x_i^0(k) - x_i^0(k)}{\max x_i^0(k) - \min x_i^0(k)}$$

To calculate the grey relational coefficients (GRCs) below equations is used,

$$\xi_i(k) = \frac{\Delta_{min} + \xi\ \Delta_{max}}{\Delta_{0i}(k) + \xi\ \Delta_{max}}$$

GRG values are calculated by the following equation,

$$\gamma_i = \frac{1}{n}\sum_{k=1}^{n} \xi_i\ (k)$$

It can be concluded from Table 8 that the grey relation grade for the first combination is rank 1.

Scanning Electron Microscopy

For the functions of many aluminum goods to be met, surface quality is crucial. It may affect a product's performance with respect to coating adhesion, corrosion resistance, and bond durability. Signals generated by an electron beam's interaction with a sample surface are used in scanning electron microscopy (SEM). The interaction volume of the electron beam within the sample is where the signal is gathered. The voltage applied to speed up the electrons in a sample gives the interaction volume for the sample.

Table 7: Normalized Values

S. No.	*Average thickness (mm) higher is better*	*Average Ra (μm) lower is better*	*Hardness (HV) higher is better*
1	1	1	1
2	0.314285714	0.72034384	0.857142857
3	0.614285714	0.01203438	0.571428571
4	0.757142857	0.33409742	0.214285714
5	0.057142857	0.28137536	0.214285714
6	0.185714286	0.11575931	0.142857143
7	0.485714286	0.22979943	0
8	0	0	0.071428571

Table 8: GRG and rank

S. No.	*Grey-relational grade*	*Rank*
1	1	1
2	0.613590956	2
3	0.479668979	4
4	0.49693937	3
5	0.381907385	6
6	0.370021565	7
7	0.406643233	5
8	0.338888889	8

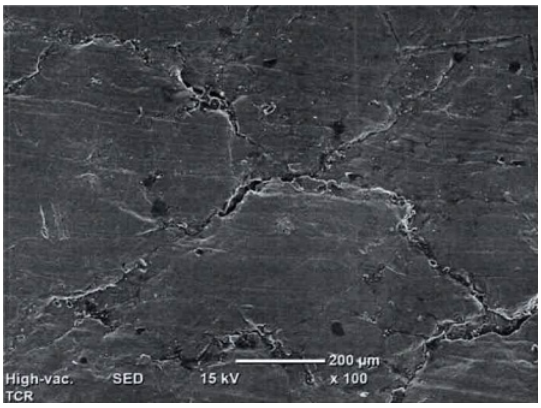

Figure 12: SEM image of specimen no. 1 at X100

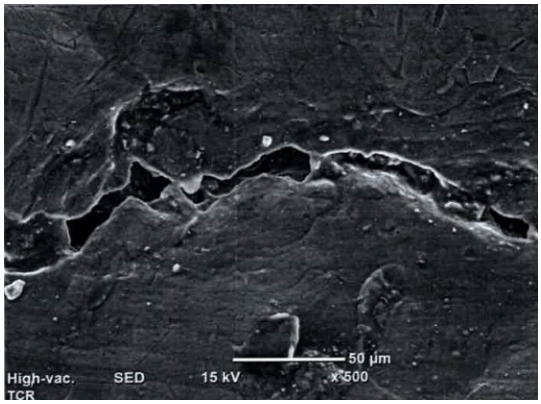

Figure 13: SEM image of specimen no. 1 at X500

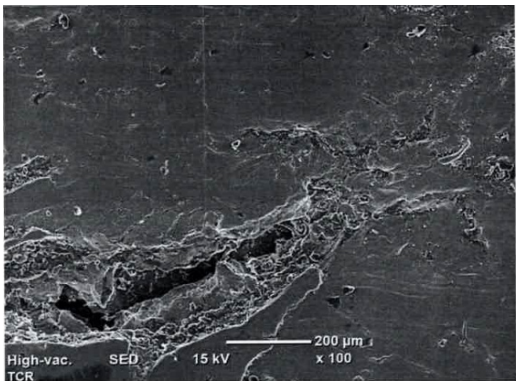

Figure 14: SEM image of specimen no. 4 at X100

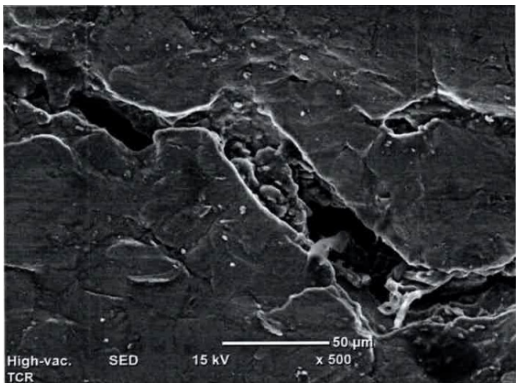

Figure 15: SEM image of specimen no. 4 at X500

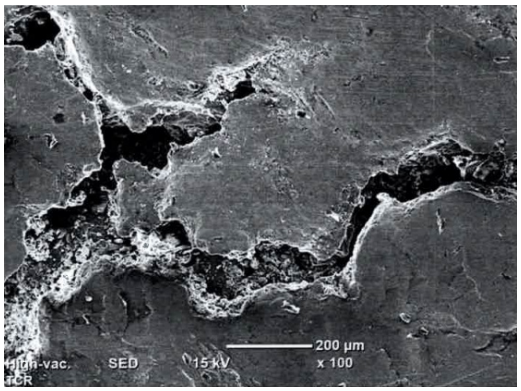

Figure 16: SEM image of specimen no. 8 at X100

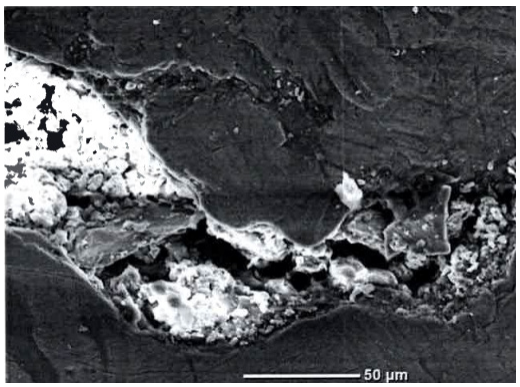

Figure 17: SEM image of specimen no. 8 X500

This provides a thorough grasp of the factors that matter and the reasons behind surface/interface failures in testing and use for aluminum goods. Figures 12 to 17 show the SEM images of the formed samples no. 1, 4, and 8, respectively.

Conclusion

The tooling needed for the DM stretching mode is currently being produced, and experiments are being conducted in accordance with the DoE plan for the DM stretching mode to observe the effects of various process factors. Wall thickness change was measured with a CMM and evaluated. This study shows that the wall thickness of the created feature is significantly influenced by incremental step depth, spindle speed, feed rate, and tool diameter. The compensating approach can be implemented using data to attain the desired or uniform thickness required for the parts to function properly. The following are the findings from the investigation:

Thickness Variation

- It is discovered that the floor bends at the beginning of the forming process, and then the thickness decreases. The formed cone has a constant thickness at its base.
- Based on the plots, it can be deduced that a reduction in tool diameter, spindle speed, increased feed rate, as well as incremental step depth results in a decrease in thickness variation.
- There is a greater loss in thickness at higher spindle speeds, and for less variance in wall thickness, a larger feed rate is advised.
- Because the material's formability declines with increasing incremental step depth, incremental step depth has a greater impact on variations in wall thickness.
- Lower tool diameters can result in less wall thickness reduction; this is possible because smaller tools are more formable and provide a higher resultant force.
- This data might help apply various compensating strategies to achieve uniform thickness.
- More research in the area of thickness compensating technique is possible.

Surface Roughness

- The reactions are greatly impacted by feed rate, tool diameter, spindle speed, and incremental step depth.
- Spindle speed and tool diameter are the next most significant factors affecting surface roughness, after-feed rate, and incremental step depth.
- Surface roughness rises with rising incremental step depth as well as surface roughness rises with rising feed rate as well.
- In comparison to feed rate and incremental step depth, surface roughness is less significantly impacted by spindle speed and tool diameter.
- This information could help achieve the appropriate surface finish for the form pieces to work properly.

Hardness

- It is discovered that the floor bends at the beginning of the forming process, which is followed by a decrease in thickness, and finally, the thickness stays constant at the base of the formed cone.
- From the main effect plot, it is found incremental step depth is the most significantly impacting the hardness followed by feed rate.
- Spindle speed and tool diameter do not significantly affect the hardness.
- As Incremental step depth increases, hardness decreases. At the lower value of incremental step depth, we have maximum hardness.
- This data may be helpful to get desired or uniform hardness for deformation machining forming.

Grey Relation Analysis

- This multi-objective optimization technique is used to determine how response variables and process parameters relate to one another. The best possible parameter combination will be determined by evaluating the highest GRG.
- The largest value of GRA is achieved at the 1st run order with incremental step depth of 0.08 mm, feed rate of 2000 mm/minute, spindle speed of 40 rpm, and tool diameter of 6 mm. Thus, the process of this combination optimizes thickness variation, surface roughness, and hardness.

SEM Analysis

SEM analysis shows a predominant amount of cracking and voids at higher levels of parameters, i.e., Sample 08. This leads to the formation of uneven surface patterns or non-uniformity of the surface. Sample No. 1 with a feed rate of 2000 mm/minute, spindle speed of 40 rpm, incremental step depth of 0.08 mm, and tool diameter of 6 mm gives better voids and cracks on the surface compared to the two samples.

Future Scope

The current study has demonstrated that to achieve the appropriate surface quality during deformation machining, it is significant to investigate the effects of process parameters. Moreover, it is demonstrated that process parameter optimization can be effectively achieved through the use of GRA-based analysis. The SEM of the surface gives clear evidence that the specimens fail at the higher level of parameters. The further exploration of this is to check the feasibility of the process for different materials for different shapes and responses.

References

Agrawal, A., Ziegert, J., Smith, S., Woody, B., & Cao, J. (2012). Study of dimensional repeatability and fatigue life for deformation machining bending mode. Journal of Manufacturing Science

and Engineering, 134(6), 1–12.

Ambrogio, G., De Napoli, L., Filice, L., Gagliardi, F., & Muzzupappa, M. (2005). Application of Incremental Forming process for high customised medical product manufacturing. Journal of Materials Processing Technology, 162-163(SPEC. ISS.), 156–162.

Ambrogio, G., Gagliardi, F., Bruschi, S., & Filice, L. (2013). On the high-speed Single Point Incremental Forming of titanium alloys. CIRP Annals - Manufacturing Technology, 62(1), 243–246.

Ambrogio, G., Gagliardi, F., & Filice, L. (2013). Robust design of incremental sheet forming by taguchi's method. Procedia CIRP, 12, 270–275.

Azaouzi, M., & Lebaal, N. (2012). Tool path optimization for single point incremental sheet forming using response surface method. Simulation Modelling Practice and Theory, 24, 49–58.

Bhattacharya, A., Maneesh, K., Venkata Reddy, N., & Cao, J. (2011). Formability and surface finish studies in single point incremental forming. Journal of Manufacturing Science and Engineering, 133(6).

Filice, L., Fratini, L., & Micari, F. (2002). Analysis of material formability in incremental forming. CIRP Annals - Manufacturing Technology, 51(1), 199–202.

Jagtap, R., Kashid, S., Kumar, S., & Hussein, H. M. A. (2015). An experimental study on the influence of tool path, tool diameter and pitch in single point incremental forming (SPIF). Advances in Materials and Processing Technologies, 1(3-4), 465–473.

Jeswiet, J., Duflou, J. R., Szekeres, A., & Lefebvre, P. (2005). Custom Manufacture of a Solar Cooker – A Case Study. Advanced Materials Research, 6-8, 487–492.

Jeswiet, J., Micari, F., Hirt, G., Bramley, A., Duflou, J., & Allwood, J. (2005). Asymmetric single point incremental forming of sheet metal. CIRP Annals - Manufacturing Technology, 54(2), 88–114.

Jeswiet, J., & Young, D. (2005). Forming limit diagrams for single point incremental forming of aluminium sheet. Proceedings of the Institution of Mechanical Engineers, Part B: Journal of Engineering Manufacture, 219(4), 359–364.

Malhotra, R., Reddy, N. V., & Cao, J. (2010). Automatic 3D spiral toolpath generation for single point incremental forming. Journal of Manufacturing Science and Engineering, 132(6), 1–10.

Parmar, P. L., & George, P. M. (2021). Effect of Process Parameters on Wall Thickness Variation in Deformation Machining Stretching Mode. International Journal of Mechanical Engineering, 6(3), 1713–1719.

Silva, M. B., Skjoedt, M., B Journal ay, N., & Martins, P. A. F. (2009). Revisiting single-point incremental forming and formability/failure diagrams by means of finite elements and experimentation. Journal of Strain Analysis for Engineering Design, 44(4), 221– 234.

Singh, A., & Agrawal, A. (2014). Comparison of Dimensional Repeatability and Accuracy for Deformation Machining Stretching Mode with Sheet Metal Components. Design and Research Conference (AIMTDR 2014), AIMTDR, 1–5.

Singh, A., & Agrawal, A. (2015a). Experimental investigation on elastic spring back in deformation machining bending mode. ASME 2015 International Manufacturing Science and Engineering Conference, MSEC 2015, 1(April).

Singh, A., & Agrawal, A. (2015b). Investigation of surface residual stress distribution in deformation machining process for aluminum alloy. Journal of Materials Processing Technology, 225(April), 195–202.

Singh, A., & Agrawal, A. (2016a). Comparison of deforming forces, residual stresses and geometrical accuracy of deformation machining with conventional bending and forming. Journal of Materials Processing Technology, 234(April), 259–271.

Singh, A., & Agrawal, A. (2016b). Investigations on structural thinning and compensation stratagem in deformation machining stretching mode. Manufacturing Letters, 9, 1–6.

Singh, A., & Agrawal, A. (2017). Experimental force modeling for deformation machining stretching mode for aluminum alloys. Sadhana - Academy Proceedings in Engineering Sciences, 42(2), 271–280.

Singh, A., & Agrawal, A. (2018). Investigation of Parametric Effects on Geometrical Inaccuracies in Deformation Machining Process. Journal of Manufacturing Science and Engineering, Transactions of the ASME, 140(7).

Smith, G. S., Woody, B., Ziegert, J., & Huang, Y. (2007). Deformation machining - A new hybrid process. CIRP Annals - Manufacturing Technology, 56(1), 281–284.

Smith, J., Malhotra, R., Liu, W. K., & Cao, J. (2013). Deformation mechanics in single-point and accumulative double-sided incremental forming. International Journal of Advanced Manufacturing Technology, 69(5-8), 1185–1201.

Smith, K. S., Us, N. C., & Wmdy, B. A.-. (2009). U S Patent (19) United States (12). 19.

Smith, S., & Dvorak, D. (1998). Tool path strategies for high speed milling aluminum workpieces with thin webs. Mechatronics, 8(4), 291–300.

Tlusty, J., Smith, S., & Winfough, W. R. (1996). Techniques for the Use of Long Slender End Mills in High-speed Milling. CIRP Annals - Manufacturing Technology, 45(1), 393–396.